Experimental and Simulation Studies on the Transport of Argon in Polycarbonate Membranes

Mar López-González,[†] Enrique Saiz,[‡] Julio Guzmán,[†] and Evaristo Riande*[,†]

Instituto de Ciencia y Tecnología de Polímeros (CSIC), 28006 Madrid, Spain, and Departamento de Química-Física, Universidad de Alcalá, Alcalá de Henares, Madrid, Spain

Received November 14, 2000; Revised Manuscript Received February 5, 2001

ABSTRACT: The transport of argon in membranes of poly(bisphenol A carbonate-*co*-4,4′-(3,3,5-trimethylcyclohexylidene)diphenol carbonate), under differences of pressure, Δp, lying in the interval 8−160 cmHg and in the temperature range 30−55 °C, is described. The experimental values of the permeability and diffusion coefficients at 30 °C and $\Delta p = 76$ cmHg are 4.5 barrers and 3.0×10^{-8} cm^2 s^{-1}, respectively. The values of these parameters are nearly independent of the differences of pressure between the two faces of the membrane. The permeability and the diffusion coefficients obey Arrhenius behavior with activation energies of 3.7 and 6.7 kcal mol^{-1}, respectively. The permeation of argon in the membranes was simulated using the transition-state approach. Good agreement between simulated and experimental results is found by assuming that the polymer chains of the membrane fluctuate around equilibrium positions with a root-mean-square deviation Δ of 0.3 Å at 40 °C. Comparison of the experimental and simulated values for the diffusion and solubility coefficients suggests that the value of Δ increases with temperature at a rate of 0.005 Å K^{-1}.

Introduction

In the past decades, considerable attention has been paid to the studies of the intrinsic permeation properties of polymers as a consequence of the ever growing use of these materials for permselective membranes for gas separation, protective coatings, and food packing. Gas transport is governed by the solubility and diffusion coefficients of gases in the membranes. Gas sorption mainly entails thermodynamic interactions between the permeant and the matrix, while the diffusive step depends on both the volume of the permeant and the mobility of the molecular chains integrating the membranes. Therefore, the diffusion and sorption processes will be affected by the thermodynamic states of the membranes: semicrystalline, glassy, and rubbery.

Owing to the cooperative micro-Brownian motions occurring in polymer chains in the rubbery state, a high density of nonpermanent holes is present in the membranes into which the permeant molecules can easily jump. The holes have in most cases a volume high enough so that the discrimination in the diffusion process by effect of the permeant size is rather poor. The gas selectivity of rubbery membranes is strongly dependent on the sorption process, and for light gases the logarithm of the solubility coefficient is a linear function of the critical temperature.[1,2]

As a result of the frozeness of micro-Brownian motions below the glass transition temperature, the glassy state is better suited than the rubbery state to discriminate gases in their transport in membranes. In low free volume glassy polymers, diffusivity selectivity is often higher than in rubbery polymers. Systematic studies carried out on the diffusivity of small weakly interacting molecules in a great deal of glassy membranes show that the fractional free volume, v_g, strongly determines this process. There is, however, a polymer dependence that seems to arise mainly from the chain stiffness and the cohesive energy.[3−6] Faupel and coworkers[7] have suggested an activation barrier, in addition to the barrier for overcoming the attractive forces between diffusant and polymer. This barrier cannot be incorporated into the preexponential factor in the equation that expresses the diffusion coefficient in terms of the exponential of the reciprocal of the free volume.

In principle, new insights into the mechanisms of diffusion of small molecules in membranes could be provided by molecular dynamics methods. These techniques allow the simulation of the trajectories of the diffusants in the matrix and the determination of the diffusion coefficients from the trajectories. However, computing time may be prohibitively large to monitor the transport of gases in membranes in the glassy state. Actually, a significant fraction of computing time is spent by the diffusing molecules moving in holes that do not contribute to the diffusion until conditions appear that allow jumping of the diffusants to neighboring holes. However, refinements developed in molecular dynamics lately led to the transition-state theory[8] that allows the prediction of barrier properties of polymers in the glassy state in a reasonable computing time.

In our laboratories efforts are being made aimed to the critical interpretation of the transport of gases in membranes in the glassy state as a function of their structure. Polycarbonate polymers exhibit good properties for gas separation[7,9−14] because they combine high selectivity and large throughput, presumably due to the large distributions of pockets of available volume with respect to other polymers.[15−17] Pursuing in the objective of relating structure and transport properties, we report in this work the experimental values of the permeation and diffusion coefficients of argon in membranes prepared from poly[bisphenol A carbonate-*co*-4,4′-(3,3,5-trimethylcyclohexylidene)diphenol carbonate], whose repeating unit has the structure schematically represented in Figure 1. It is expected that the 3,3,5-trimethylcyclohexylidene moiety hinders chains packing efficiency. This not only will impede the development

[†] Instituto de Ciencia y Tecnología de Polímeros.
[‡] Universidad de Alcalá.

10.1021/ma0019508 CCC: $20.00
Published on Web 06/06/2001

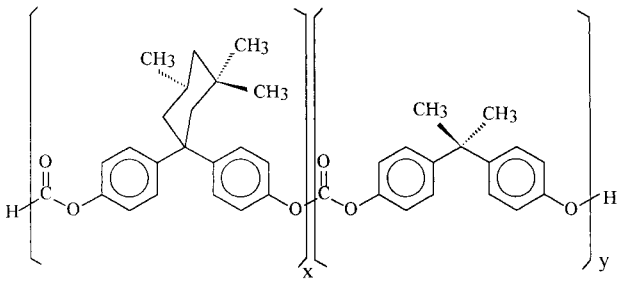

Figure 1. Schematic representation of the repeating unit of the polymer used to prepare the polycarbonate membrane.

of crystallinity but also will increase the permeability of the membranes to gases. Finally, both the diffusion and permeability coefficients of argon in the polycarbonate membranes were computed using simulation methods and the results compared with the experimental values.

Experimental Section

Poly[bisphenol A carbonate-*co*-4,4′-(3,3,5-trimethylcyclohexylidene)diphenol carbonate] in pellets form supplied by Aldrich was used as received. The fractions of the two components of the copolymer measured by NMR spectroscopy were roughly similar. The polycondensation process ensures a random distribution of the two comonomers. The glass transition temperature of the polycarbonate, measured with a Perkin-Elmer DSC-7 calorimeter, was 205 °C. This value corresponds to the temperature at the onset of the departure of the endotherm from the baseline in the glassy region. Because of the insolubility of the polymer in polar solvents of high volatility, such as methylene chloride, films of thickness 132 ± 3 μm were prepared by compression molding at 300 °C of pellets of polycarbonate. The films were kept under compression at this temperature for 15 min, and then they were quenched at room temperature.

The permeation of argon through the films was measured with an experimental device described in detail elsewhere.[18] In short, the permeation cell is made up of two chambers separated by the membrane. The pressure of the diffusant at the upstream chamber was measured with a Gometrics transducer working in the 0−10 bar range. The evolution of the pressure with time in the downstream chamber was also measured with a MKS-627B transducer operating in the 10^{-4}–1 mmHg interval. The permeation cell was immersed in a thermostat set at the temperature of interest. Before each experiment, the inlet of air into the evacuated downstream chamber was measured as a function of time and further subtracted from the curves representing the pressure of the permeant vs time in the downstream chamber.

Results

An illustrative plot showing the variation of the pressure $p(t)$ of argon in the downstream chamber with time is shown in Figure 2. The plot shows a transient zone at short times followed by a region at long times in which the pressure is a linear function of time. The evolution of the pressure of the permeant in cmHg with time in the downstream chamber is described by[19]

$$p(t) = 0.2786 \frac{p_0 ALST}{V} \times \left(\frac{Dt}{L^2} - \frac{1}{6} - \frac{2}{\pi^2} \sum_{n=1}^{\infty} \frac{(-1)^n}{n^2} \exp\left(- \frac{Dn^2\pi^2 t}{L^2} \right) \right) \quad (1)$$

where p_0 is the pressure in cmHg of the gas at the upstream chamber, V is the volume in cm^3 of the downstream chamber, and A and L are respectively the area in cm^2 and the thickness in cm of the film. The solubility S and diffusion D coefficients are given respectively in [cm^3 (STP)/cm^3 cmHg] and cm^2/s. In steady-state condition ($t \rightarrow \infty$), eq 1 becomes

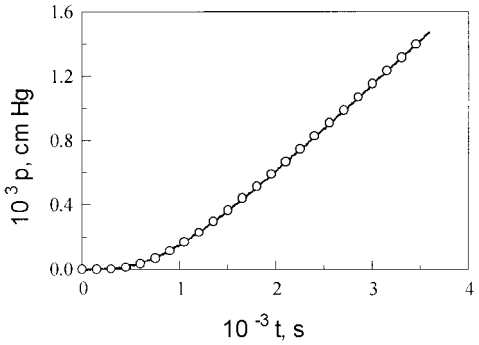

Figure 2. Experimental (continuous line) and calculated values (○) of the evolution of the pressure of argon with time in the downstream chamber. $T = 30$ °C.

$$p(t) = 0.2786 \frac{p_0 ALST}{V} \left(\frac{Dt}{L^2} - \frac{1}{6} \right) \quad (2)$$

The plot of $p(t)$ against t in steady-state conditions is a straight line intercepting the time axis at $(D\theta/L^2) - {}^1/_6 = 0$, where θ is the time lag. Accordingly,

$$D = \frac{L^2}{6\theta} \quad (3)$$

This method was suggested long time ago by Barrer[20] to obtain the diffusion coefficient from permeation measurements. Since the permeability coefficient, P, is the product of the solubility coefficient times the diffusion coefficient, the value of P in barrers {1 barrer = [10^{-10} cm^3 (STP) cm/(cm^2 s cmHg)]} can be obtained from eq 1 giving

$$P = 3.59 \frac{VL}{p_0 AT} \lim_{t \rightarrow \infty} \frac{\mathrm{d}p(t)}{\mathrm{d}t} \quad (4)$$

where V, L, and A are given in units of the cgs system and p_0 and $p(t)$ in cmHg.

Values at different temperatures of the permeability coefficient, calculated by means of eq 4, are plotted as a function of the pressure of the upstream chamber, p_0, in Figure 3. It can be seen that the permeability coefficient is rather insensitive to p_0 in the range of pressures studied. The results for the diffusion coefficient, obtained from eq 3, are plotted as a function of p_0 in Figure 4. With the exception of the isotherm corresponding to the lower temperature, the diffusion coefficient slightly decreases with increasing upstream pressure.

The values of P and D were used in eq 1 to obtain the pressure in the downstream chamber as a function of time. In general, the results obtained for $p(t)$ fit very well the experimental results as can be seen in Figure 2 where, for illustrative purposes, the experimental and calculated values of the pressure of the downstream chamber are shown as a function of time.

The temperature coefficient of the permeability, diffusion, and solubility coefficients in the temperature range that does no span significant thermal transitions in the polymer can be described by two Arrhenius

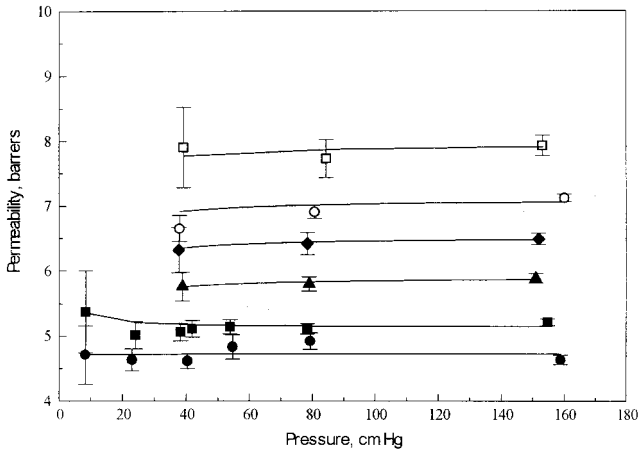

Figure 3. Dependence of the permeation coefficient of argon on the pressure of the upstream chamber at different temperatures: (●) 30, (■) 35, (▲) 40, (◆) 45, (○) 50, and (□) 55 °C.

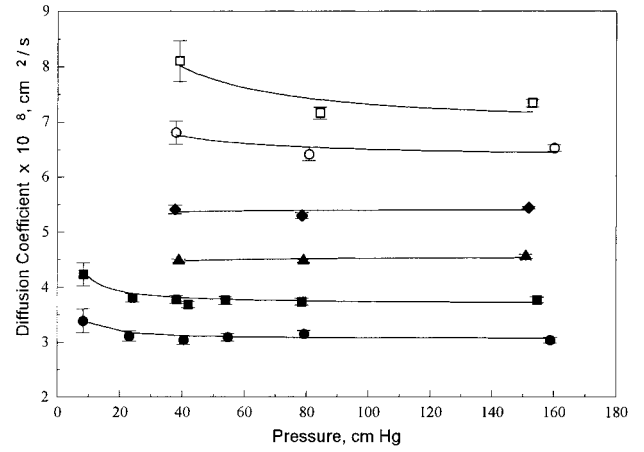

Figure 4. Variation of the diffusion coefficient of argon with the pressure of the upstream chamber at different temperatures: (●) 30, (■) 35, (▲) 40, (◆) 45, (○) 50, and (□) 55 °C.

expressions and a van't Hoff equation

$$P = P_0 \exp(-E_P/RT)$$

$$D = D_0 \exp(-E_D/RT)$$

$$S = \frac{P}{D} = S_0 \exp(-H_S/RT) = \frac{P_0}{D_0} \exp[(E_D - E_P)/RT] \tag{5}$$

where P_0, D_0, and S_0 are preexponential factors, E_P and E_D are respectively the apparent activation energies of the permeability and diffusion coefficients, and $H_S = E_P - E_D$ is the heat of sorption. The activation energy for permeation is the sum of a kinetic parameter, E_D, and a thermodynamic parameter, H_S. Accordingly, the more exothermic is the solution of the gas in the matrix, less effect will the temperature have in the gas permeation through the membrane. Arrhenius plots for the permeability and diffusion coefficients of argon are shown in Figure 5. The values obtained for E_P and E_D at $p_0 = 1$ bar were 3.70 and 6.70 kcal mol^{-1}, respectively, so the heat of sorption was -3.00 kcal mol^{-1}. The activation energies associated with the permeation and diffusion processes do not show a definite dependence on pressure. The average values of E_P and E_D in the interval of pressures 0.5−2 bar were respectively 4.01 ± 0.22 and 7.19 ± 0.45 kcal mol^{-1}.

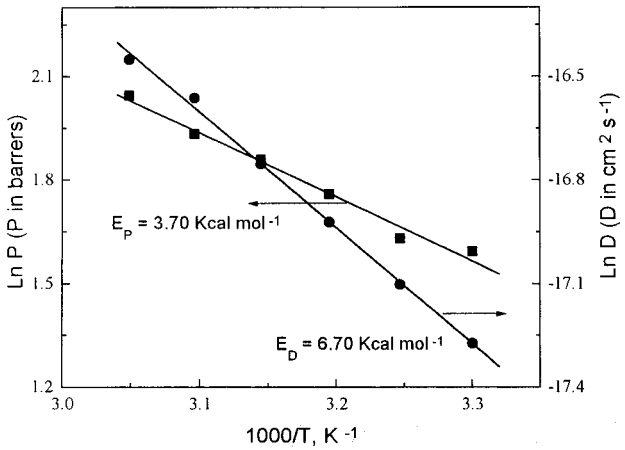

Figure 5. Arrhenius plots for the permeability and diffusion coefficients of argon in the membrane.

Molecular Dynamics Simulations

Theoretical Calculation of the Diffusion Coefficient. The diffusion coefficient, D, can be calculated by means of the so-called Einstein relationship[8,18,21]

$$D = \frac{1}{6} \lim_{t\to\infty} \left\{ \frac{\partial}{\partial t} \langle (\mathbf{r}(t) - \mathbf{r}(0))^2 \rangle \right\} \tag{6}$$

where $\mathbf{r}$ is the vector position of the diffusant particle within the polymeric host matrix.

Molecular dynamics (MD) procedures may be employed to simulate the trajectories followed by a diffusant guest particles inside a host polymeric matrix, thus providing a direct procedure to evaluate D according to eq 6. However, the molecular systems required for these simulations are quite large, and hence the calculations require an enormous amount of computer time that drastically reduces the maximum time span that can be reached by this procedure. A direct consequence of this limitation is that the application of eq 6, which requires prohibitively large computing time to reach the steady-state condition, may be questionable.

This difficulty can be avoided by using the transition-state approach (TSA)[8,18,21] whose main assumption is that the diffusant path is independent of the structural relaxations of the polymeric matrix. Thus, the atoms of the matrix are assumed to have fixed equilibrium positions and are only allowed to fluctuate around those positions with a root-mean-square deviation Δ, customarily referred to as smearing factor. The probability of finding a deviation δ between actual and equilibrium positions of any given atom within the polymeric matrix is[8]

$$W(\delta) \sim \exp\left(-\frac{\delta^2}{\Delta^2}\right) \tag{7}$$

The diffusant particle is then allowed to statistically jump among the sites contained in the fixed matrix, defined as the positions in which the interaction among the particle and the matrix is a local minimum and therefore represent positions where the probability of finding the diffusant is maximum. Simulated time spans on the order of milliseconds can be easily reached with this approach.

Molecular Dynamics Software. The DL_POLY package[22,23] was employed for all the MD simulations described below. A time step of 1 fs (i.e., 10^{-15} s) was

used for integration of the equations of motion. The AMBER force field[24−27] was employed to compute conformational energies. Coulombic potentials were evaluated as the interactions among partial charges assigned to every atom of the system by means of the MOPAC package and the AM1 procedure[28] with a distance-dependent function; i.e., the effective dielectric constant of the system was set equal to the distance between the interacting atoms. Cutoff distances $r_c = 9.6$ and 8 Å were used respectively for Coulombic and van der Waals interactions, i.e., interactions between atoms i and j were set to zero when their distance r_{ij} is larger than the appropriate r_c.

Molecular Systems. Four H-terminated oligomers, such as those shown in Figure 1 (i.e., 3288 atoms in total, $M = 23\,637$ g/mol), were packed into a cubic box having periodic boundary conditions (PBC) and a box side length $L = 33.98$ Å. This arrangement provided a density of ca. 1.10 g cm^{-3}. The system was generated within the box by adding one unit at the time and minimizing the energy after each addition by means of a simplex procedure that explored the rotations over all single bonds in the sample while keeping constant the values of bond lengths and bond angles. A series of annealing processes were then applied to the sample thus generated. Each one of those processes consisted of 50 000 steps MD simulation carried out under NVT conditions with an Evans thermostat. This means that atomic velocities were scaled after each MD step to give the exact desired value of T, thus avoiding large thermal fluctuations that may be produced when the interatomic forces become large. All the internal coordinates of the sample (i.e., bond lengths, bond angles, and rotations) were allowed to fluctuate during these processes while the temperature was slowly raised from 1 to 500 K and lowered again to 1 K. The resulting structure was finally optimized with respect to all its internal coordinates by means of a conjugated gradient method until the rms value of the force gradient was smaller than 0.1 kcal/Å, thus providing the polymeric host matrix that will be used in all the calculations described below.

TSA Strategy. Once the polymeric host matrix was prepared, the guest diffusive atom was successively placed at the $N = 10^6$ positions obtained by gridding the cubic lattice with 100 intervals on each side.[8,18,21] The interaction between host matrix and guest atom was evaluated and employed to compute the probability of finding the guest atoms at every one among those N positions. The grid points were then assigned to sites that are defined as the local minima of the energy function (or local maxima on the probability) by means of a steepest descendent gradient algorithm started at each grid point that ends into the site were the starting grid point belongs. The partition function of each site depends on both its depth and extent, i.e., the value of the energy at the bottom and the number of grid points that belongs to it, and determines the mean residence time for the guest atom in the site.

Unfortunately, the evaluation of the conformational energy at the grid points is not as accurate as it would be desirable for a good performance of the minimization procedure. Consequently, some odd results may be obtained as a close inspection of the sites obtained reveals. Thus, some fake sites too small as to hold a single diffusant particle appear close to a much larger site with a crest surface between them too low as to be a real barrier. In fact, those fake sites are produced by roughness in the energy surface that fools the minimization procedure. Fake sites were eliminated in the present calculation, and their corresponding grid points were incorporated to their neighbor main sites.

On the other hand, in some cases the crest surface separating some pairs of neighbor sites may be too small as to allow the passage of a diffusant particle having a given van der Waals radius r_{vdW} and therefore a cross section $S_D = \pi(r_{vdW})^2$. To account for this effect, the rate constant R_{ij} of diffusant transition from site i to adjacent site j was weighted with a factor W_{ij} that takes into account the relative values of the crest surface and the cross section of the diffusant particle. Thus

$$W_{ij} = \frac{\delta_{ij}}{S_D} \tag{8}$$

where δ_{ij} was taken to be zero when the crest surface between sites i and j is smaller than S_D and unity otherwise.

The rate of diffusant transitions from site i to site j is then

$$R_{ij} = W_{ij}\left(\frac{kT}{8\pi m}\right)^{1/2}\frac{Z_{ij}}{Z_i} \tag{9}$$

where k is Boltzmann's constant, m is the mass of the diffusant, Z_{ij} is the configurational partition function at the crest surface separating sites i, j, and Z_i is the partition function for the valley of site i. The probability for the $i \rightarrow j$ transition is then

$$p_{ij} = \tau_i R_{ij} \tag{10}$$

with τ_i being the mean residence time for the guest atom in site i:

$$\tau_i = \frac{1}{\sum_n R_{in}} \tag{11}$$

where the sum expands over all the sites adjacent to i.

The diffusion process is then simulated by a random walk of the diffusant within the polymeric matrix.[8,18,21] The walk consists of a series of jumps from one initial site to a neighbor site that is designated as target. Each jump is assumed to require a time equal to the main residence time of the initial site. The first initial site is randomly chosen among all the sites of the matrix, and the target site is randomly selected according to the probabilities dictated by the crest surface between initial and target sites. The target site of the first jump is taken as initial site for the second jump, for which a new target is chosen among the neighbor sites. The walk continues until a predetermined time span (normally of the order of milliseconds) is reached. All the results shown below are averages over 500 independently generated walks.

The solubility S of the diffusant gas in the host polymeric matrix was evaluated as[8]

$$S = \frac{1}{kTV}\int \exp\left(-\frac{E}{RT}\right) \mathrm{d}V = \frac{1}{kT}\left(\frac{Z}{N}\right) \tag{12}$$

where k is Boltzmann's constant, V the volume of the polymeric matrix, and N the number of grid points employed to compute the partition function Z.

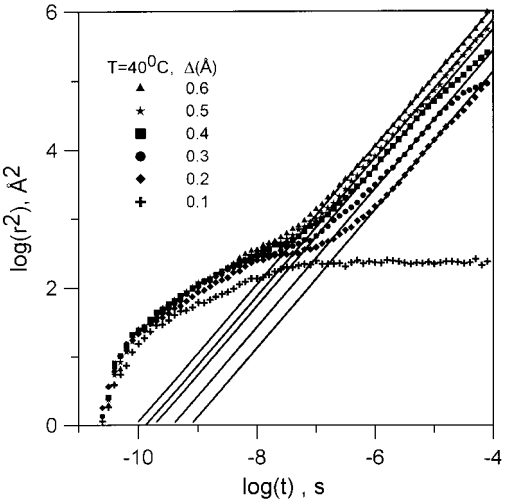

Figure 6. Double-logarithmic plot of the time dependence of the squared displacement $\mathbf{r}^2$ of an Ar atom diffusing within the polymeric matrix according to the TSA scheme. The calculations were performed at 40 °C with several values of the smearing factor Δ.

Thus, the units of S are given by the reciprocal of kT when it is computed as the ratio (Z/N). Employing molar quantities under STP conditions, $RT = 76$ cmHg cm^3 [cm^3 (STP)]$^{-1}$ and therefore

$$S = \frac{Z}{76N}\left(\frac{\text{cm}^3\,(\text{STP})}{\text{cm}^3\,\text{cmHg}}\right) \qquad (13)$$

which are the units employed in the present work.

Results and Discussion

Figure 6 shows a double-logarithmic plot of the displacement of the diffusant atom $\mathbf{r}^2$ vs time computed at 40 °C as a function of the smearing factor Δ. As the curves in Figure 6 indicate, the variation of $\mathbf{r}^2$ with time is strongly time-dependent. However, the diffusive regime in which $\mathbf{r}^2$ is roughly linear with time is eventually reached at times of the order of 10^{-7} s in most cases, provided that Δ > 0.1 Å. When time and displacement become large, a downturn with a slope smaller than unity is obtained, which probably is due to the limited size of the PBC box. Values reported below for Δ > 0.1 Å were computed by fitting the linear variation or $\mathbf{r}^2$ with t. Those fittings are represent by straight lines in Figure 6.

It seems that when Δ is too small, the diffusive regime is not reached. An estimation of the value of D may then be obtained by taking the ratio between the displacement and the time spent to reach it and average the result over the few last points of the simulation. Values reported below for Δ = 0.1 Å were obtained on this way, and even if they may be affected by a rather large error, the exact values are not important for our purposes because only Δ ≈ 0.3 Å provides values in the range of experimental results.

Figure 7 represents the values of the solubility S, diffusion D, and permeability P coefficients computed at 40 °C as a function of Δ. As this figure indicates, the smearing factor has a very strong effect on the three magnitudes. The solubility coefficient decreases with increasing values of Δ that represent larger oscillations of the atoms on the polymeric matrix, thus decreasing the free space allowed to the guest atoms. However, the diffusion coefficient increases very strongly with increasing Δ because the oscillations favor the opening of passages from one site to another. It is unfortunate that an exact determination of Δ becomes virtually impossible. However, rough estimates based on the thermal oscillations of the host atoms[18,29] suggest a range of values around 0.3−0.4 Å. As shown in Figure 7, for Δ ≈ 0.3 Å the theoretical values are in rather good agreement with the experimental ones.

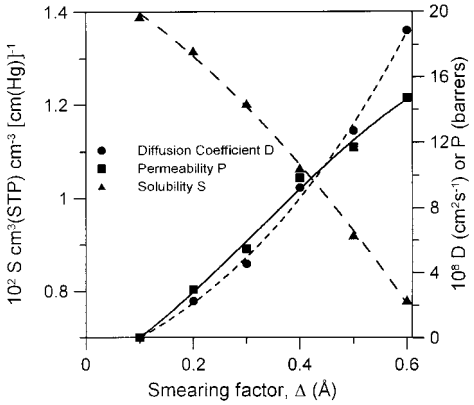

Figure 7. Values of the diffusion D, solubility S, and permeability P coefficients obtained at 40 °C as a function of the smearing factor Δ. The lines represent least-squares fittings and are included only to show the shape of the variation.

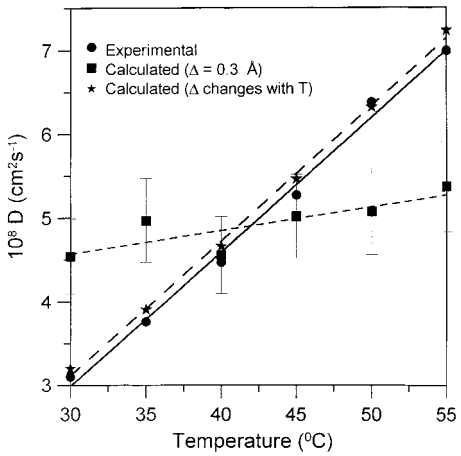

Figure 8. Variation with temperature of the experimental and calculated values of D. The lines represents least-squares fitting and are included only to show the shape of the variation. The squares represent theoretical results obtained employing Δ = 0.3 Å while the stars are values computed with Δ = 0.29 Å at 40 °C and increasing with temperature at a rate of 0.005 Å/K. The error involved in the calculation of D was estimated to be ca. 10% as is indicated by the vertical bars in one of the theoretical set of results.

The temperature dependence of D obtained with this scheme is not very good as can be seen in Figure 8 where theoretical and experimental values are compared. While experimental values increase more than twice over the 25 °C interval of temperatures covered in this work, theoretical results computed with a fixed value of Δ = 0.3 Å are roughly temperature independent. This behavior may be due to limitations of the TSA approach that produce uncertainties on the value of D that are larger than the variation produced by changing the temperature. But it also may be due to the fact of employing a fixed, temperature-independent, value of Δ. This parameter represents the difference between the speed of the oscillations on the host and the displace-

ment of the guest atoms. Both kinds of motions become faster as temperature increases. It could be postulated that the increase in atomic velocities might be higher for the host atoms that are lighter than the diffussant atoms so that Δ could slightly increase with T. And in fact, a rather small variation of Δ with T would bring agreement between theory and experience. Actually, the stars in Figure 8 represent theoretical values computed for $\Delta = 0.29$ Å at 40 °C, assuming that this parameter increases with T at a rate of 0.005 Å/K.

The rather high solubility coefficient of argon and other gases in polycarbonate membranes is presumably promoted by the combination of a long, flat, and rigid segment with a significant packing inhibiting segment.[30] It has been suggested that the coexistence of regions of well-packed environments having relatively low local free volume in communication with local environments of relatively unoccupied volume distributed as packing defects may provide an optimum level topography for high selectivity and flow.[31]

Conclusions

The present study shows that the diffusion and permeability coefficients of argon in glassy poly[bisphenol A carbonate-*co*-4,4′-(3,3,5-trimethylcyclohexylidene)-diphenol carbonate] are independent of the pressure of the upstream chamber in the range of pressures 8−160 cmHg. This behavior suggests a low diffusant-matrix affinity coefficient, and as a result, the apparent solubility coefficient obeys Henry's law in the interval of pressures indicated.

In this study the rate constant of diffusant transition from site *i* to adjacent site *j* is weighted by a factor that takes into account the relative values of the surface at the crest potential between the two sites and the cross-sectional area of the diffusant particle. The simulations give a good account of the experimental transport coefficients provided that the smearing factor that accounts for the fluctuations of the chains around a mean position has a value of ca. 0.3 Å, the same as that in many other systems.[18,21,32] Comparison of the simulated and experimental results suggests that the smearing factor might increase with temperature at a rate of ca. 0.005 Å K^{-1}.

Acknowledgment. This work was supported by the CAM and the DGESIC through the Grants DTM/0069/1998 and PB97-0778, respectively.

References and Notes

(1) Toi, K.; Morel, G.; Paul, D. R.; Flory, P. J. *J. Appl. Polym. Sci.* **1982**, *27*, 2987.
(2) VanKrevelen, D. W. *Properties of Polymers: Their Correlation with Chemical Strucutre*; Elsevier: Amsterdam, 1990.
(3) Meares, P. *J. Am. Chem. Soc.* **1954**, *76*, 3415.
(4) VanAmerongen, G. J. *Rubber Chem. Technol.* **1964**, *37*, 1065.
(5) Brandt, W. W. *J. Phys. Chem.* **1959**, *63*, 1080.
(6) Petropoulos, J. H. In *Polymeric Gas Separation Membranes*; Paul, D. R., Yampolskii, Y. P., Eds.; CRC Press: Boca Raton, FL, 1994; pp 17−81.
(7) Thran, A.; Kroll, G.; Faupel, F. *J. Polym. Sci., Part B: Polym. Phys.* **1999**, *37*, 3344.
(8) Gusev, A. A.; Müller-Plathe, F.; van Gunsteren, W. F.; Suter, U. W. *Adv. Polym. Sci.* **1994**, *116*, 207.
(9) Muruganandam, N.; Paul, D. R. *J. Membr. Sci.* **1987**, *34*, 185.
(10) Hellums, M. W.; Koros, W. J.; Husk, G. R.; Paul, D. R. *J. Appl. Polym. Sci.* **1991**, *43*, 1977.
(11) Hellums, M. W.; Koros, W. J.; Husk, G. R.; Paul, D. R. *J. Membr. Sci.* **1989**, *46*, 93.
(12) Hellums, M. W.; Koros, W. J.; Husk, G. R. *Polym. Mater. Sci. Eng., Proc. ACS Div. Polym. Mater. Sci.* **1989**, 378.
(13) Hellums, M. W.; Koros, W. J.; Schmidhauser, J. C. *J. Membr. Sci.* **1992**, *67*, 75.
(14) Grüger, A.; Gotthardt, P.; Pönitsch, M.; Brion, H. G.; Kirchheim, R. *J. Polym. Sci., Part B: Polym. Phys.* **1998**, *36*, 483.
(15) Gentile, T.; Arizzi, S.; Suter, U. W.; Ludovice, J. P. *Ind. Eng. Chem. Res.* **1995**, *34*, 4193.
(16) Royal, J. S.; Torkelson, J. M. *Macromolecules* **1992**, *25*, 4792.
(17) Arizzi, S.; Mott, P. H.; Suter, U. W *J. Polym. Sci., Part B: Polym. Phys.* **1992**, *30*, 415.
(18) Laguna, M. F.; Guzmán, J.; Riande, E.; Saiz, E. *Macromolecules* **1998**, *31*, 7488.
(19) Crank, J. *The Mathematics of Diffusion*; Oxford University Press: Oxford, 1975.
(20) Barrer, R. M. *Trans. Faraday Soc.* **1939**, *35*, 628.
(21) Laguna, M. F.; Guzmán, J.; Saiz, E.; Riande, E. *J. Chem. Phys.* **1999**, *110*, 3200.
(22) Forester, T. R.; Smith, W. DL_POLY (Ver. 2.10), Daresbury Laboratory, Daresbury, Warrington WA4 4AD, England.
(23) Allen, M. P.; Tildesley, D. J. *Computer Simulation of Liquids*; Clarendon: Oxford, 1987.
(24) Weiner, S. J.; Kollman, P. A.; Case, D. A.; Singh, U. C.; Ghio, C.; Alagona, G.; Profeta, S.; Weiner, P. *J. Am. Chem. Soc.* **1984**, *106*, 765.
(25) Weiner, S. J.; Kollman, P. A.; Nguyen, D. T.; Case, D. A. *J. Comput. Chem.* **1986**, *7*, 230.
(26) Homans, S. W. *Biochemistry* **1990**, *29*, 9110.
(27) Cornell, W. D.; Cieplak, P.; Bayly, C. L.; Gould, I. R.; Merz, K. M.; Ferguson, D. M. D.; Spellmeyer, C.; Fox, T.; Caldwell, J. W.; Kollman, P. A. *J. Am. Chem. Soc.* **1995**, *117*, 5179.
(28) MOPAC, *Quantum Chemistry Program Exchange*, Department of Chemistry, Indiana University, Bloomington, IN.
(29) Gusev, A. A.; Suter, U. W. *J. Chem. Phys.* **1993**, *99*, 2228.
(30) Muruganandam, N.; Koros, W. J.; Paul, D. R. *J. Polym. Sci., Part B: Polym. Phys.* **1987**, *25*, 1999.
(31) Koros, W. J.; Walker, D. R. B. *Polym. J.* **1991**, *23*, 481.
(32) López-González, M.; Guzmán, J.; Saiz, E.; Riande, E. Submitted for publication.

MA0019508